A CONCRETE SOLUTION

ROELENS Carla, SOFIA Ugo and STRIMBU-LEE Arthur

March 2025

our supervising teachers:

Mr. Fisher-Côte, Mr. Barbier and Mr. Boudoyen

THE TEAM

Tenacious. That's how we describe ourselves. Perseverance. That's how we define our mindset. We come from a Physics Olympiad group composed of six students. Since our defeat at the inter-academic final in Nancy in December 2024, we have been improving our subject and developing a new aspect. Passion and a taste for scientific approach pushed us not to stop and to present ourselves to the CGénial competition. So this is who we are.

(a) ROELENS Carla (video and university contact)

(b) SOFIA Ugo (research and calculations)

(c) STRIMBU-LEE Arthur (writing and coding)

"I love the research process and working on concrete allows me to see a practical application of our work." - ROELENS Carla

"Passionate about science, I love learning more. This project has really allowed me to expand my horizons and discover new fields." - SOFIA Ugo

"I've always loved math and coding. The Python code was interesting to program and I discovered LaTeX, which I love!" - STRIMBU-LEE Arthur

Acknowledgments

We would like to thank our physics and mathematics teachers Mr. Fischer-Côte, Mr. Boudoyen and Mr. Barbier who accompanied us throughout our research process. We also thank Professor Jan Lagerwall and doctoral student Yosuke Pestana Nakamura from the University of Luxembourg for taking the time to advise us and answer our questions, as well as our parents for their encouragement and unwavering support throughout the project.

1 Introduction

Reinforced concrete is a composite material widely used in many types of infrastructure such as bridges or schools. Its use has become widespread in the 20th century, particularly for its strength and durability. We can cite the remarkable works of Le Corbusier who was the architect of two monuments listed as UNESCO World Heritage sites: The Radiant City of Marseille (Figure 1.a) and the Villa Savoye in Poissy (Figure 1.b).

(a) The Radiant City in Marseille

(b) The Villa Savoye in Poissy

Figure 1: Reinforced concrete constructions by Le Corbusier

However, after visiting the Radiant City of Marseille, we noticed cracks of varying sizes in several areas of its structure, including its pillars (Figure 2). After some research, we understood that the carbonation phenomenon was occurring within the reinforced concrete. This progressive degradation of reinforced concrete represents a danger for the infrastructure. After this visit, we immediately established a connection between this problem and our Olympiad subject.

Figure 2: Crack observed on a pillar of the Radiant City of Marseille

We are students at Vauban, French School of Luxembourg (Figure 3) and our school was also built with reinforced concrete. Its construction dates from 2020 and does not yet show cracks like those of the Radiant City of Marseille which dates from 1952.

Figure 3: Vauban, French School of Luxembourg

Research questions: **How can we preserve a reinforced concrete infrastructure and slow down or even stop its degradation? How can the application of paint prevent cracks in a concrete structure? How can connecting an entire building to a generator save it?**

We will answer these questions in this paper and our team will present (with all humility) how to save Vauban!

2 Evaluation of reinforced concrete degradation

2.1 What is reinforced concrete?

2.1.1 Formation of reinforced concrete

Reinforced concrete is an assembly of concrete structured by steel bars (Figure 4). These two components of reinforced concrete have their own interest and advantages.

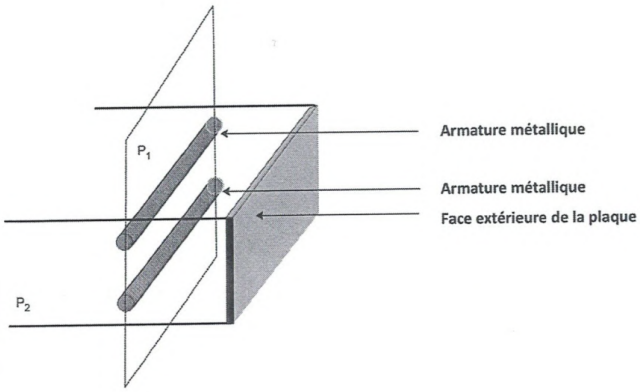

Figure 4: Diagram of reinforced concrete

Concrete is composed of cement, aggregates[1] and water. Cement being a hydraulic binder, it hardens when in contact with water in a process called hydration. It is similar to dicalcium silicate with the chemical formula Ca_2SiO_4.

We can therefore express the formation of concrete by the following chemical reaction:

$$2\,Ca_2SiO_4(s) + 4\,H_2O(l) \longrightarrow Ca_3Si_2O_7, 3\,H_2O(s) + Ca(OH)_2(s)$$

Calcium hydroxide ($Ca(OH)_2$) produced is a strong base. It makes the concrete basic through water, and its pH is between 12 and 14.

[1] composed of sand or gravel

2.1.2 Physical properties of reinforced concrete

Concrete withstands compressive forces very well but poorly withstands tensile forces, and consequently, flexural forces. This is a problem since infrastructure must also be able to resist tension and flexion. Steel, on the other hand, withstands tensile and flexural forces very well. Its addition to concrete to make reinforced concrete is therefore justified.

2.2 Creation of our reinforced concrete

We carried out several tests for creating reinforced concrete, the manufacturing protocol of which you will find in Appendix A. However, we first had to find the quantities of mortar and water to use to create the strongest concrete. We therefore created eight different concretes using 60 grams of mortar for each sample and between 0 and 35mL of water at intervals of 5mL from one sample to the next (Figure 5).

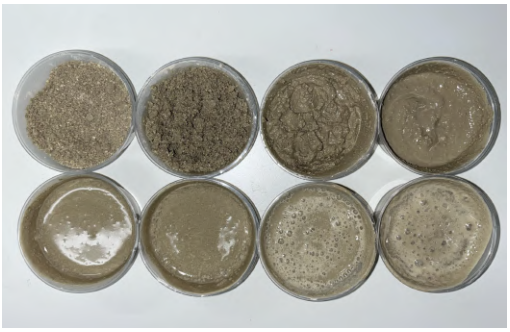

Figure 5: Our eight concrete samples

After letting our preparations dry for 24 hours, we noticed that the concretes with water quantities of 0, 5, and 10mL were too powdery and had not even really solidified, while the samples with 30 and 35mL were very fragile and disintegrated at the slightest touch. Among the concretes with water quantities of 15, 20, and 25mL, the concrete with 15mL of water was the most solid and compact, less pasty than the others. We deduced that we need a mass concentration of mortar in water of:

$$Cm = \frac{m}{V}$$

$$\Leftrightarrow Cm = \frac{60\,g}{15 \times 10^{-3}\ \text{mL}}$$

$$\Leftrightarrow Cm = 4 \times 10^{3} \text{g} \cdot \text{L}^{-1}$$

We learned that the concretes used in buildings are classified into different categories. The NF EN 206/CN standard categorizes concretes into three groups according to their density:

- Light concrete: ρ between 800 and 2000 kg/m^3
- Normal concrete: ρ between 2000 and 2600 kg/m^3
- Heavy concrete: $\rho > 2600$ kg/m^3

Our concrete is composed of 60g of mortar and 15mL of water which weighs 15g, so 75×10^{-3} kg. The volume of our concrete is 35mL, or $35 \times 10^{-6} m^3$. Therefore, the density of our concrete is equal to:

$$\rho_{\text{concrete}} = \frac{75}{35}$$

$$\rho_{\text{concrete}} = 2140\,\text{kg/m}^3$$

Our concrete can therefore be categorized among normal concretes. All the concretes we created subsequently, reinforced or not, were created using the optimal mass concentration of mortar demonstrated. To evaluate its basicity, we used phenolphthalein (Figure 6). This is an acid-base indicator that is colorless when the pH of the medium studied is less than 9 and pink when it is equal to or greater than 9.

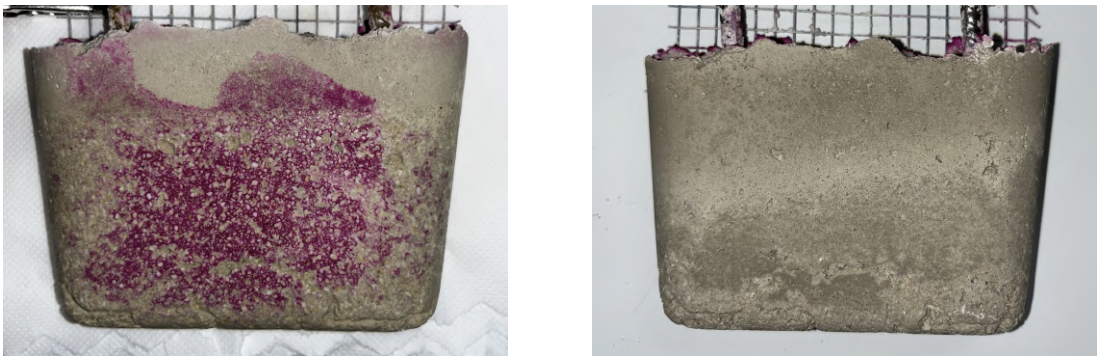

(a) Basic reinforced concrete (b) Acidified reinforced concrete

Figure 6: Phenolphthalein tests: on the left the basic reinforced concrete, on the right the acidified reinforced concrete

2.3 Carbonation

Over time, all concrete undergoes an aging phenomenon. This is carbonation. Indeed, carbon dioxide (CO_2) present in the atmosphere diffuses into the concrete through its pores and dissolves there thanks to the water present. During carbonation, carbon dioxide will dissolve calcium hydroxide which we can write:

$$Ca(OH)_2(s) \longrightarrow Ca^{2+}(aq) + 2\,HO^-(aq)$$

The carbonation reaction therefore causes calcium hydroxide to react with carbon dioxide to form calcium carbonate and water. The other chemical species making up the concrete are spectators. This is why they are not represented in the following chemical equation:

$$Ca^{2+}(aq) + 2\,HO^-(aq) + CO_2(aq) \longrightarrow CaCO_3(s) + H_2O\,(l)$$

As mentioned previously, calcium hydroxide ($Ca(OH)_2$) present in concrete is responsible for its basic character. We highlighted this with the dissolved form of $Ca(OH)_2$ which presented hydroxide ions (OH^-), responsible for the basicity of a solution. We notice that after the carbonation reaction, the hydroxide ions have disappeared. When calcium hydroxide has been completely consumed, the concrete becomes acidic.

When concrete becomes acidic, the layer that protects the steel is no longer stable. By breaking down, this layer allows moisture to corrode the steel reinforcement (Figure 7). When the reinforcement is heavily corroded, the corrosion products can swell, degrade the concrete and cause cracking or breakage (Figure 2 - Radiant City of Marseille).

Figure 7: Example of the consequences of corrosion due to carbonation (rust)

2.4 Study of the rigidity of two concretes

Before proposing solutions to save reinforced concrete constructions, we need to ensure that acidified concrete, otherwise known as "aged", is less resistant to forces applied to it than basic concrete, called "young".

We did not include steel reinforcement in our experiment since we were only seeking to evaluate the strength of acidic and basic concrete. To evaluate their strength, we calculated their Young's modulus. We therefore created two concretes of

the same concentration (see part **2.2**) and subjected them to compressive forces. The principle is to place the concrete being tested between the jaws of the press. Then we turn the crank of the press while measuring the number of turns in degrees. But first, we measured the height of our identical concretes using calipers (Figure 8). We measured 15.7mm.

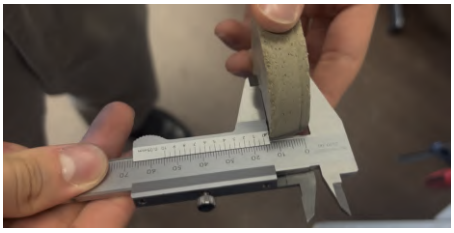

Figure 8: Measurement of the height of the two concretes

Figure 9 illustrates our setup.

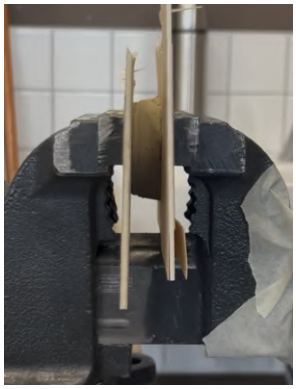

(a) View of the concrete deformation

(b) View of the rotation angle of the press crank

Figure 9: Setup of our experiment to calculate Young's modulus

In our case, the modulus of elasticity also called Young's modulus is a quantity that expresses the rigidity of concrete as a function of the stress exerted on it. Young's modulus is expressed by:

$$E = \frac{\sigma}{\varepsilon}$$

with E the Young's modulus in Pa, σ the stress in Pa and ε dimensionless and expressible by $\frac{d}{l_0}$

The stress can be expressed by $\frac{F}{A}$ which are respectively the force applied to the contact surface A $= 8 \times 10^{-3} m^2$. Our setup allows us to calculate the force F using the following formula:

$$F = \frac{C\theta}{d}$$

with **C** the torque which is a constant in our calculation, θ the angle of rotation of the crank in degrees and **d** the difference in height of the concrete $l_0 - l$ after compression

To recap, our setup provides us with all the information necessary to calculate this modulus: **C** the torque which is a constant that we will replace with 1 since we have not calculated it (this will not affect the results of the calculation), $\boldsymbol{\theta}$ the angle of rotation of the press crank in degrees, $\boldsymbol{l_0}$ the initial height of our concrete in m, **l** the final height of the concrete in m and **d** the difference between the initial height of the concrete and the height after compression in m. Finally, the formula we will use to calculate the Young's modulus of acidic and basic concrete is:

$$E = \frac{\sigma}{\varepsilon}$$

$$\Leftrightarrow \quad E = \frac{\frac{F}{A}}{\frac{d}{l_0}}$$

$$\Leftrightarrow \quad E = \frac{\frac{\frac{C \times \theta}{d}}{A}}{\frac{d}{l_0}}$$

$$\Leftrightarrow \quad E = \frac{\frac{C \times \theta \times l_0}{d}}{A \times d}$$

$$\Leftrightarrow \quad \mathbf{E = \frac{C \times \theta \times l_0}{A \times d^2}}$$

Finally, we conducted experiments on a basic concrete, called "young" and an acidic concrete, called "old". The results are shown in Figure 10. The acidic concrete was acidified in hydrochloric acid with a molar concentration C = 1mol/L. We turned the crank 90° for both tests. Then, we measured the difference **d** of the two concretes:

- $d_{\mathbf{basic}} = 15.7 - 13 = 2.7$ mm
- $d_{\mathbf{acidic}} = 15.7 - 12.7 = 3$ mm

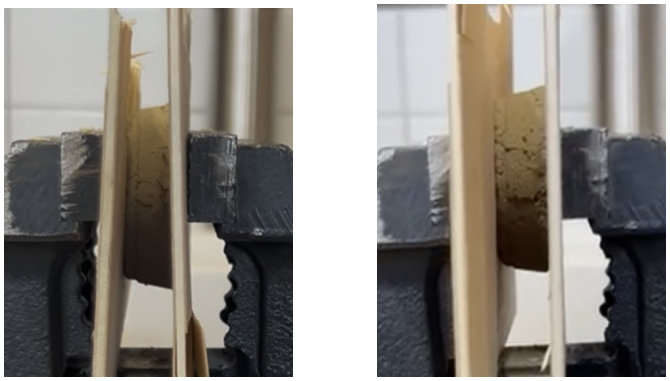

(a) Basic concrete (b) Acidic concrete

Figure 10: Results of the Young's modulus experiment

We then calculated the Young's modulus of the two concretes with the following results:

$$E_{basic} = \frac{C \times \theta \times l_{0basic}}{A \times {d_{basic}}^2} \quad \text{and} \quad E_{acidic} = \frac{C \times \theta \times l_{0acidic}}{A \times {d_{acidic}}^2}$$

$$E_{basic} = \frac{90 \times 15.7}{8 \times 10^{-3} \times 2.7^2} \quad \text{and} \quad E_{acidic} = \frac{90 \times 15.7}{8 \times 10^{-3} \times 3^2}$$

$$E_{basic} \approx \mathbf{24} \text{ MPa} \quad \text{and} \quad E_{acidic} \approx \mathbf{19} \text{ MPa}$$

Therefore 24 MPa >19 MPa, and we can conclude by confirming our hypothesis advanced at the beginning of this part: acidic concretes are less resistant than basic concretes. We can note that our concrete corresponds to a BPE[1] and almost to a BFC[2]. But now, let's look at the solutions we propose.

[1]Ready-Mix Concrete (between 16MPa and 60 MPa)
[2]On-Site Manufactured Concrete (between 25MPa and 35 MPa)

3 Prevention: liquid crystals

3.1 Introduction to liquid crystals

Matter can be categorized into three states according to the arrangement of its molecules: solid, liquid, and gaseous. This arrangement depends on the conditions to which matter is subjected, such as temperature and pressure. Liquid crystals represent a unique state of matter. Indeed, since the work of the German physicist Otto Lehmann on molten cholesterol ester, we know that the state of a liquid crystal is found halfway between that of a crystalline solid (Figure 11.a) and that of an isotropic liquid[1] (Figure 11.b). This is called the mesophase state. According to his observations, the liquid appeared birefringent[2] like a crystal.

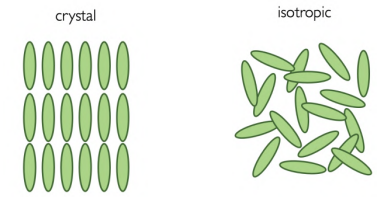

(a) Solid state of a crystal

(b) State of an isotropic liquid

Figure 11: The extreme states of a crystal

Within this mesophase state, liquid crystals are distinguished into two categories: nematics and smectics. Molecules inside a nematic liquid crystal are free to move like a liquid and orient themselves on average towards the same axis **n** (Figure 12). This orientation is a "long-range order".

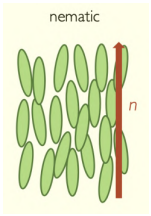

Figure 12: Nematic liquid crystal

For smectic liquid crystals, the molecules are organized in layers where they are all oriented in the same direction, either straight or diagonally (Figure 13).

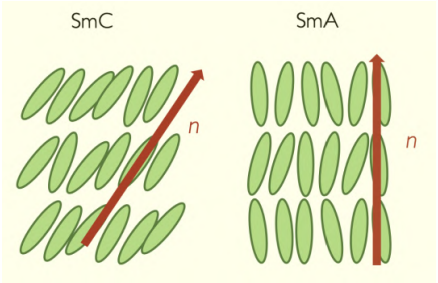

Figure 13: Smectic liquid crystal - on the left a smectic C and on the right a smectic A

This molecular organization makes nematic liquid crystals more fluid than smectics. In this thesis, we will focus on a subcategory of nematic liquid crystals: chiral nematics otherwise called cholesterics.

Cholesteric liquid crystals are nematic liquid crystals where a chiral additive has been introduced [3]. This additive gives

[1] medium in which properties are identical regardless of the direction of observation

[2] body that has two refractive indices

[3] a system is said to be chiral (derived from Greek: kheir meaning hand) if it cannot be superimposed on its mirror image in any combination of rotations and translations

the liquid crystal a helical structure. Indeed, the molecules are structured in layers[1]. The structure of liquid crystal molecules remains nematic and they are still directed towards their director **n**. Chirality implies a perpendicular rotation of this director relative to the pitch of the helix **p** (Figure 14). The pitch of the helix **p** is defined on the axis **m** by the complete rotation of the director **n**.

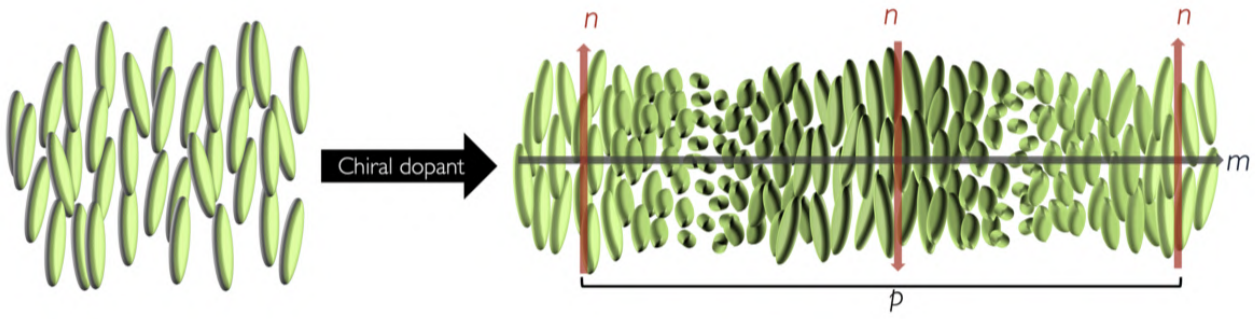

Figure 14: Diagram explaining chirality at the molecular scale of the cholesteric liquid crystal

3.2 Mechanism of color change following mechanical deformation

In a cholesteric liquid crystal, the color we see is the result of selective reflection of light by the layers of its helical structure (Figure 15). We can explain the path of light as a function of the pitch of the helix **d** and the angle of incidence $\boldsymbol{\theta}$ of the ray as in Figure 11.

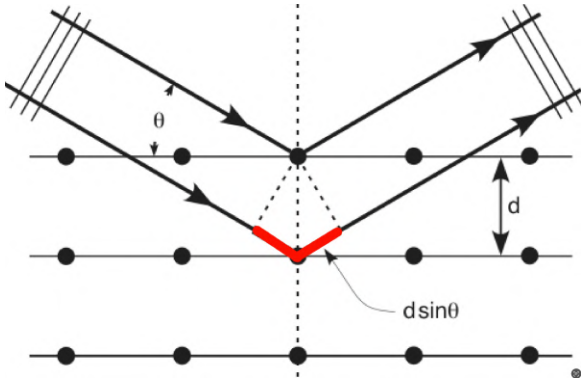

Figure 15: Diagram of the diffraction phenomenon in a crystal

The two waves reflected by the two layers of the crystal overlap, they must form constructive interference (Figure 16) for the emitted wavelength to be visible.

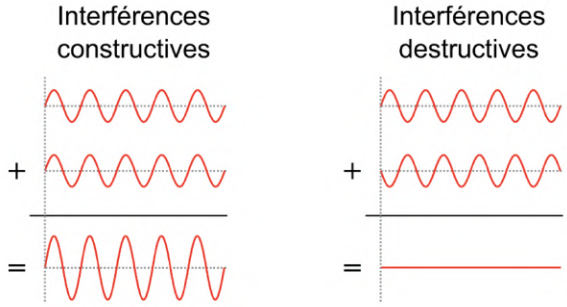

Figure 16: Diagram of constructive and destructive interference phenomena

[1] they take on the property of smectic liquid crystals which are more viscous

For interferences to be constructive, the path difference (highlighted in red in Figure 15) must be a multiple of wavelength. We can express the path difference by Bragg's law:

$$k\lambda = 2nd\sin\theta$$

with **k** a natural integer corresponding to the order of interference in the crystal plane and **n** the refractive index of the crystal.

Knowing this, we propose an experiment of applying a layer of liquid crystal on a deformable support. Since the liquid crystal is incompressible, if the support is stretched, the pitch of the helix will decrease. Figure 17 shows the phenomenon of elongation of the support and what it would cause at the molecular structure level.

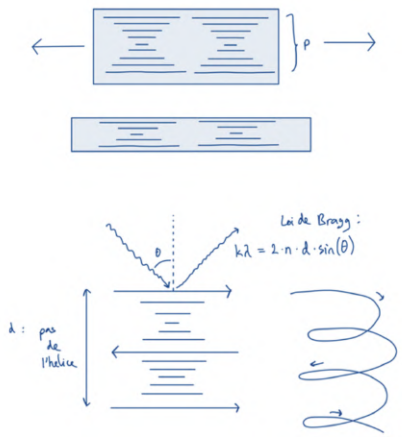

Figure 17: Diagram of the elongation of the support and its consequences at the molecular level

In practice, this should give a result as shown in Figure 18. We will now show you what we have done.

(a) Moderate tension: observed color red (∼700nm)

(b) Higher tension: observed color green (∼550nm)

Figure 18: Deformation of a liquid crystal support

3.3 Principles of our quantitative analysis

3.3.1 The approach

In our study, we aim to determine the pitch of the helix of our liquid crystal based on the color we observe. For this, we varied the color of our liquid crystal in two different ways (see section **3.4**) and took pictures of our observations. By "our" liquid crystal, we refer to the cholesteric liquid crystal paint purchased from the company SFXC (Figure 19).

Figure 19: Cholesteric liquid crystal paint from SFCX

Once the photos were taken, we had to analyze them to find the pitch of our helix. This is the complicated part of this analysis.

3.3.2 From an image to the pitch of the helix

To go from an image to the pitch of the helix, we must go through many steps. For a clearer explanation, we will go backwards, from the pitch of the helix to the image.

Suppose we need to analyze a color, which we call A.

To determine the pitch of the helix, we need the wavelength associated with color A. It can be expressed by Bragg's law which we have rearranged:

$$d = \frac{k\lambda}{2n \sin\theta}$$

To find the wavelength of color A, we will use the chromaticity diagram defined by the CIE in 1931 (Figure 20).

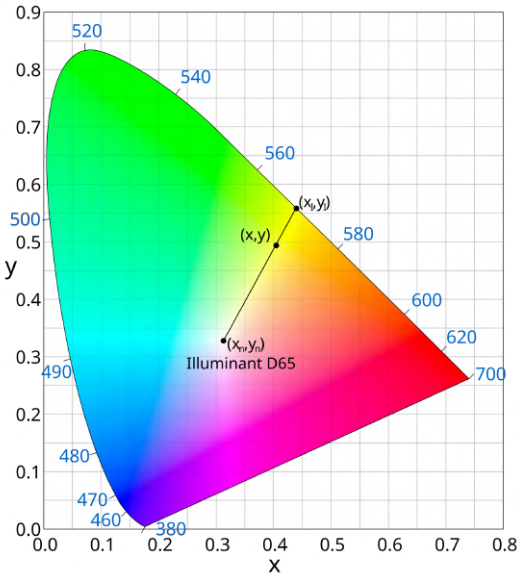

Figure 20: CIE 1931 chromaticity diagram

The curve of the diagram expresses the wavelengths of the visible on a plane (x, y). We therefore need the coordinates of the sought wavelength.

However, the coordinates (x, y) of the chromaticity diagram are only a two-dimensional representation of an XYZ space,

defined by the CIE. The coordinates (x, y) are expressed by:

$$x = \frac{X}{X+Y+Z}$$

$$y = \frac{Y}{X+Y+Z}$$

We therefore need the XYZ values of color A. Until now, the photo of our color A could only be defined with its RGB computer code. Fortunately, there is a direct link between the RGB code and the XYZ values. We need to calculate a matrix product. The RGB code can be expressed as a 3x1 matrix just like the values of the associated XYZ space. Their relationship is expressed by:

$$M \begin{bmatrix} R \\ G \\ B \end{bmatrix} = \begin{bmatrix} X \\ Y \\ Z \end{bmatrix}$$

With M the CIE RGB matrix defined by the CIE:

$$M = \begin{bmatrix} 0.49 & 0.31 & 0.2 \\ 0.17697 & 0.8134 & 0.01063 \\ 0 & 0.01 & 0.99 \end{bmatrix}$$

This is how we can go from the simple RGB code of the photo to the pitch of the helix of color A.

However, a problem remains. Liquid crystal colors are monochromatic while those of a photo are polychromatic[1]. We may find ourselves in cases where the coordinates of the plane are not on the outer curve of the diagram. They are either in the diagram, or outside and do not correspond to any theoretical wavelength[2]. To overcome this problem we have implemented the NSS[3] algorithm which looks for the point on the curve closest to the coordinates of color A. In this way, we have an approximation to within 10nm of the wavelength of color A.

In summary, we created a code that uses images of liquid crystals to determine the pitch of their helix following the presented method. Our Python code is found in Appendix B.

3.4 Our experiments

3.4.1 Mechanical deformation

We first tried to apply our liquid crystal on a deformable support so that once dried, we could stretch the belt and observe a color change. Our setup looked like Figure 21.

Figure 21: Liquid crystals applied to a deformable support

After stretching our liquid crystal belt, we did not once observe a color change (Figure 22).

[1] a computer pixel is defined by an RGB code which is a superposition of red, green and blue. This is why the photo is considered polychromatic.
[2] problem due to the polychromaticity of the image
[3] Nearest Neighbour Search

(a) Low tension: no color observed

(b) High tension: no color observed

Figure 22: Deformation of our liquid crystal belt

Then, after some research, we discovered the principle of "index matching". "Index matching" or refractive index adaptation is a process aimed at matching the refractive indices of two different media to reduce the phenomenon of light scattering at their interface. Our liquid crystal is a colloid since it is an aqueous solution in which particles of liquid crystals are suspended. These particles are small enough (<1µm) not to be visible and large enough (>1nm) to scatter the light they receive. In a colloid at the molecular scale, incident light rays are scattered by these suspended particles. This is the Tyndall effect (Figure 23).

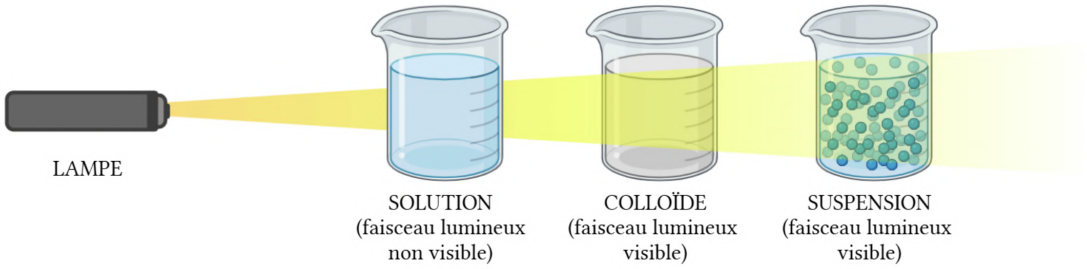

Figure 23: Diagram of the Tyndall effect

In our colloidal liquid crystal, with light being scattered, we cannot observe a color change. Index matching makes sense at this point. To be able to observe the color of our liquid crystal, we must find a fluid having the same refractive index as it, which is 1.5. This fluid prevents the scattering of light by the suspended particles. In our case, glycerol corresponds to the sought fluid with a refractive index of 1.47 which is close enough to 1.5. Figure 24 schematizes what happens at the molecular level before and after the addition of glycerol.

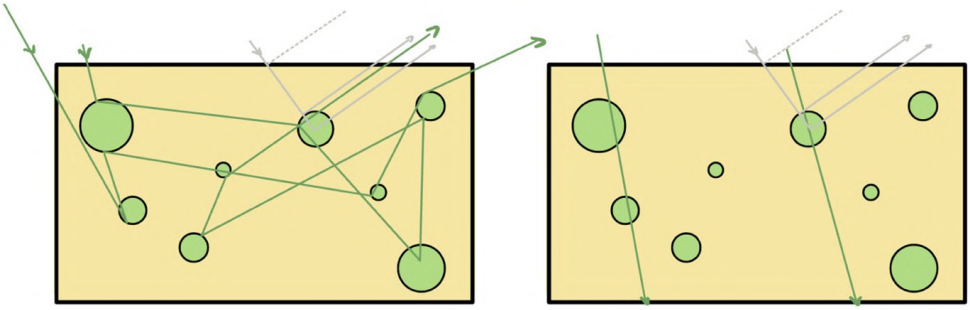

Figure 24: Diagram of the influence of glycerol application on our initial setup (before-after application)

After applying glycerol, we still could not observe a color change by stretching the belt (Figure 25).

Having found no other solutions and explanations for the constancy of the color of our belt, we called upon our partner:

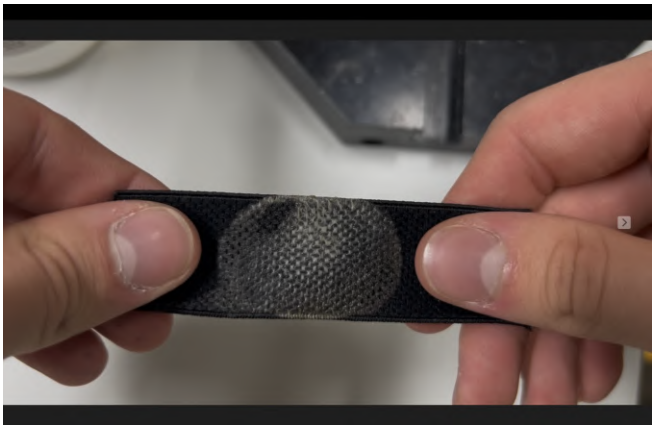

(a) Low tension: no color observed

(b) High tension: no color observed

Figure 25: Deformation of our liquid crystal belt with added glycerol

The University of Luxembourg with Professor Jan Lagerwall and doctoral student Yosuke Pestana Nakamura. Thanks to their explanations, we understood why it was impossible for us to create a liquid crystal belt ourselves. The molecules of our liquid crystal applied to the support are not polymerized, which makes it impossible to visualize the color change by mechanical deformation. This polymerization process cannot be carried out in our high school, which is why we went to create a liquid crystal belt (Figure 26) at the university, in their laboratory.

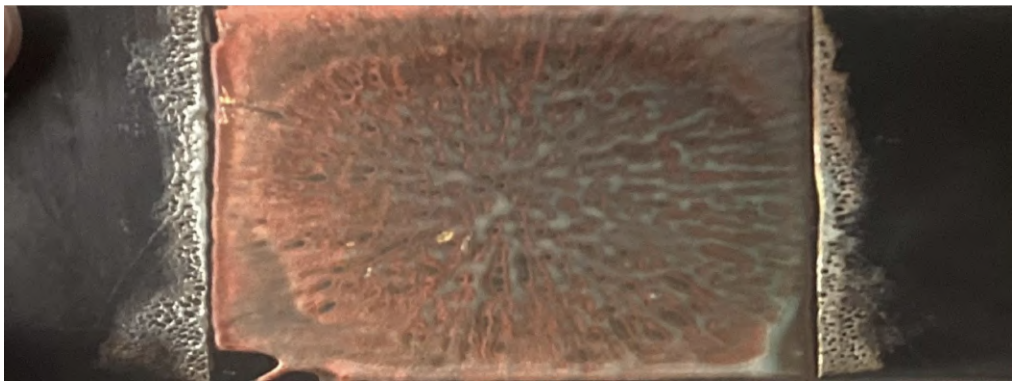

Figure 26: Belt with polymerized liquid crystals on a deformable support

Finally, we conducted our quantitative analysis of the color change of the liquid crystal belt as a function of its deformation measured by elongation. There were some steps to follow. To change the color of the belt, the pitch of the helix of the liquid crystals must vary. We therefore stretched the belt to modify the pitch of the helix. The formula for the elongation (in %) of the belt is as follows:

$$\text{Elongation} = \frac{L - LO}{LO} \times 100$$

with **L** the length of the belt (in cm) and **LO** the original length of the belt (in cm).

Then, at each step of the elongation we took a photo of the belt and entered it into our Python code to give us the pitch of the helix. To avoid imprecise values by stretching the belt by hand, we created a small machine that does it more precisely (Figure 27).

It is thus sufficient to place the two ends of our belt on the dedicated supports and to start the rail which will pull the belt. We can block the stage that interests us by placing metal bars in the structure. This allows us to take precise photos of our belt without worrying that it changes size if it is held by a human (Figure 28). We plan to improve this model so that it works automatically with a motor. The results are presented in section **3.5**.

Our first experiments on the deformable support were not useless...

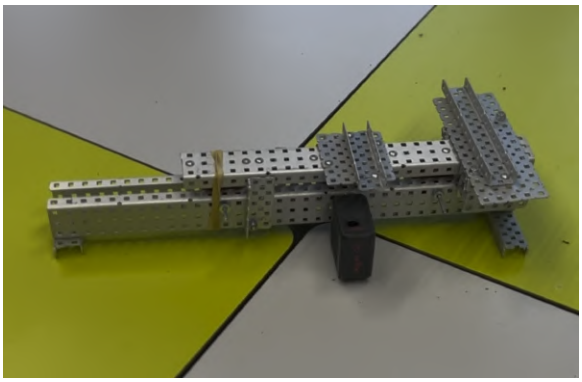

Figure 27: Machine that precisely stretches the liquid crystal belt

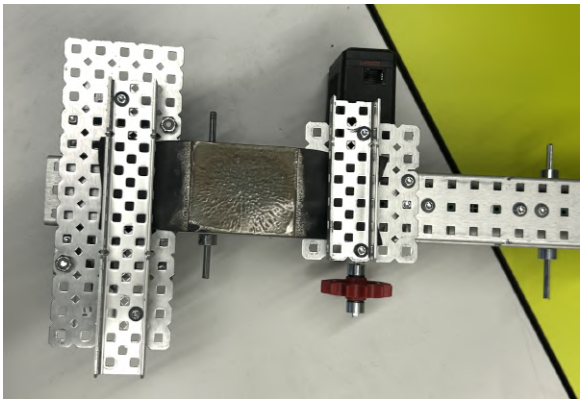

(a) Initial state of the belt machine

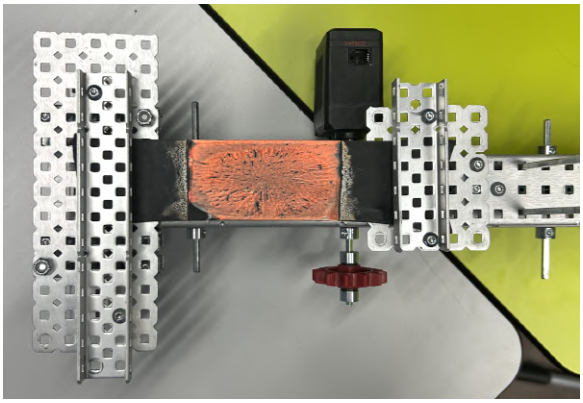

(b) State at a certain measurement of the belt

Figure 28: Demonstration of the effectiveness of elongation by the small machine

3.4.2 Temperature variation

The temperature of a liquid crystal influences the pitch of its helix. But what is the link between the first experiments where we tried to mechanically modify the pitch of the helix and the temperature of a liquid crystal? We made a lot of back and forth movements by stretching the belt, and very quickly. The mechanical energy produced by our movements was converted into thermal energy. This is why we can observe a color change of the crystal extremities after a certain time (Figure 29).

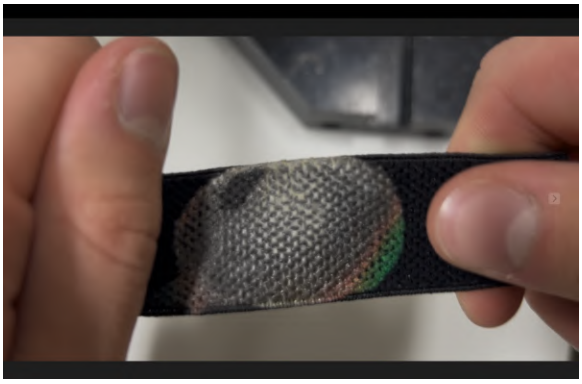

Figure 29: Our liquid crystal belt after about thirty rapid back-and-forth movements

We then noticed that the small packaging of our liquid crystal pot specified that the liquid crystals change color between 30 and 35°C. In this part, our study consists of confirming what is written on the product. Our protocol is therefore slightly different. We need to apply our liquid crystal on a rigid and larger support, to better visualize the color change.

We first applied a layer of liquid crystals on a white sheet glued to a glass plate so that the assembly was rigid. Of course, to avoid the problem of diffusion we added a layer of glycerol. We then heated this plate so that the crystal would impregnate

the sheet. As the crystal changes color between 30 and 35°C, the heat of our body is sufficient to make it change color. We heated our plate but we only saw very faint colors, almost imperceptible (Figure 30).

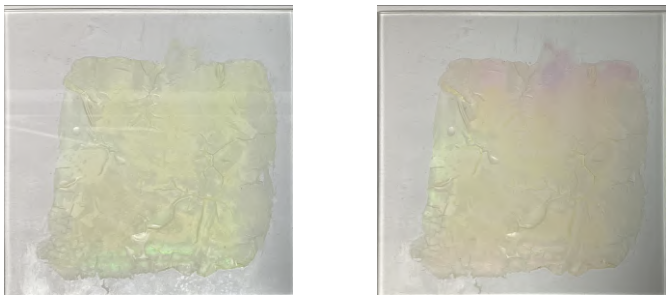

(a) Ambient temperature (b) Heated

Figure 30: Color observed by changing the heat of the plate

We then understood that the phenomenon of reflection came into play. Our liquid crystal still being a colloid, some rays pass through the crystal and are reflected by the white sheet; white sheet which returns all wavelengths of the visible spectrum. The waves reflected by the crystal and those reflected by the white sheet merge and make it very difficult to visualize the color of the liquid crystals (Figure 31).

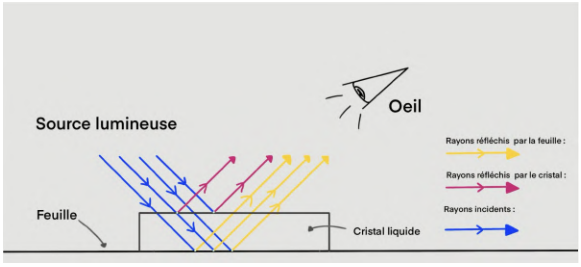

Figure 31: Diagram of the reflection phenomenon in the first setup

We therefore solved the reflection problem by changing the background of the plate to a black background, which absorbs all wavelengths. Our second setup allowed us to observe a color change as a function of temperature (Figure 32).

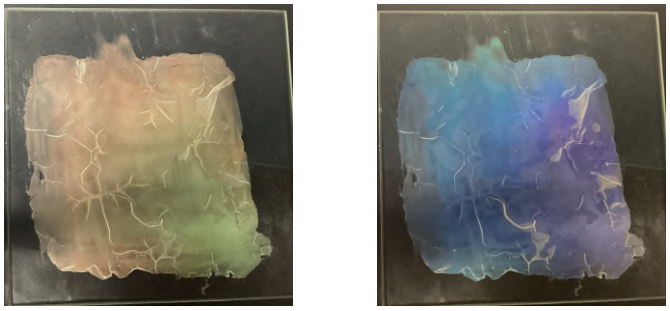

(a) Temperature of ∼26°C (b) Temperature of ∼30°C

Figure 32: Color observed by changing the heat of the plate

Thanks to our Python code and the values it returned, we were able to create the following graph which represents the pitch of the helix of our liquid crystal as a function of its temperature (Figure 33).

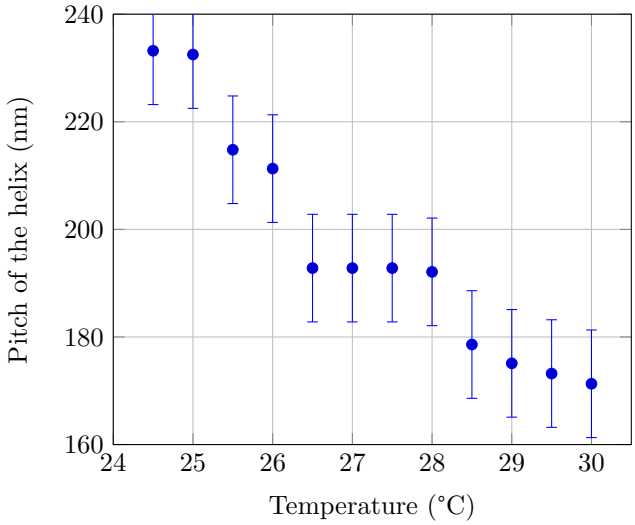

Figure 33: Evolution of the pitch of the helix as a function of temperature with an uncertainty of 10 nm

Finally, the manufacturer was not quite right since our experiments demonstrated a color variation between 24 and 30°C instead of 30 to 35°C. Although very interesting to study, changing the temperature parameter on a liquid crystal does not interest us for finding a solution to our problem.

3.5 Results and uncertainty calculations

Here are the results of our quantitative analysis by mechanical deformation (Table 1). Finally, our values with our code were so uncertain that in the design of this table, they were not interesting. We therefore used the site 405nm.com.

Elongation (%)	RGB Values	Wavelength (nm)	Pitch of the helix(nm)
35.0	193, 137, 126	630	210.0
38.3	201, 131, 118	627	209.0
41.7	213, 132, 113	621	207.0
50.0	219, 134, 106	620	206.7
56.7	221, 138, 97	615	205.0
60.0	220, 146, 89	613	204.3
68.3	217, 155, 84	610	203.3
73.3	207, 173, 80	605	201.7
76.7	199, 186, 79	601	200.3
80.0	194, 192, 81	599	199.7
83.3	187, 195, 81	557	185.7
88.3	179, 198, 82	555	185.0
90.0	175, 196, 83	554	184.7
91.7	174, 194, 83	553	184.0

Table 1: Correspondence table between elongation, RGB values, wavelengths and pitch of the helix

Figure 34 represents the color emitted by liquid crystals as a function of its elongation. We notice a considerable change in color between red and green around 80%.

These 80% represent well the cracks that concrete can present, assuming that 100% is the complete breakage of the

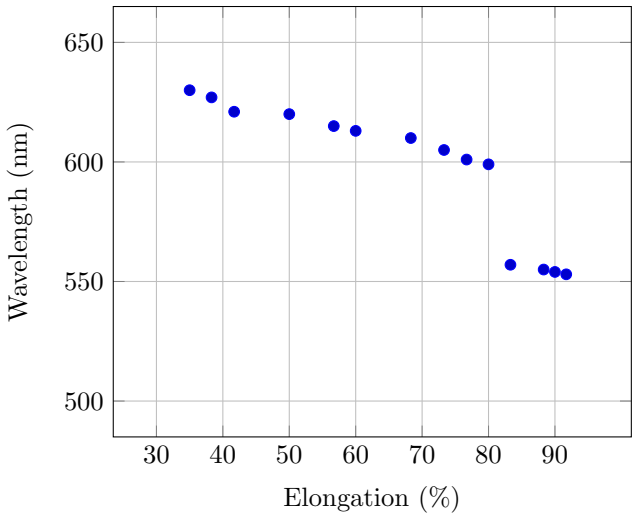

Figure 34: Wavelength as a function of elongation

concrete. Liquid crystals are therefore a very interesting solution when applied to a concrete surface to visualize and prevent cracks. Better to prevent than to cure!

4 Restoration: cathodic protection

4.1 Operation of cathodic protection

Cathodic protection against corrosion works by modifying electrical voltage relationships to reverse electrochemical reactions. When the passivation layer of steel is damaged, for example by chlorides, the electrochemical potential of the affected area shifts to more negative voltages. This creates a potential difference between the passivated and corroded areas, allowing a small current to flow, provided there is a conductive medium, in our case concrete. As in a battery, a small current flows between these two areas. The process begins at the anode, where oxygen attacks the iron, causing corrosion.
In this system, a stable iron-based anode is placed in the form of a mesh on the concrete surface, then covered with a layer of conductive mortar or concrete. Using a DC power source, a potential difference is created between the mesh, which constitutes the anode, and the reinforcement, connected to the negative pole, which acts as the cathode (Figures 35 and 36).
At the cathode, which consists of the steel reinforcement in the concrete, a water reduction reaction occurs through electrolysis, regenerating hydroxide ions according to the following equation:

$$H_2O(l) + e^- \rightarrow \frac{1}{2}H_2(g) + HO^-(aq)$$

As a result, it is not necessary to demolish the concrete layer. To ensure uniform protection, the reinforcement must be sufficiently interconnected to form an electrical network, which is generally the case with standard reinforcement arrangements.

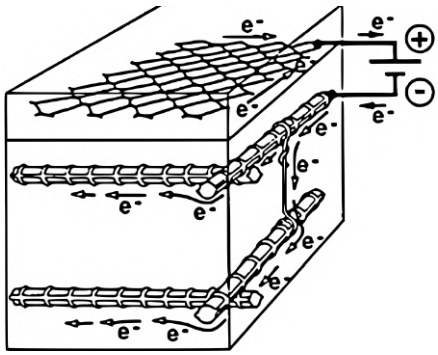

Figure 35: Cathodic protection against corrosion

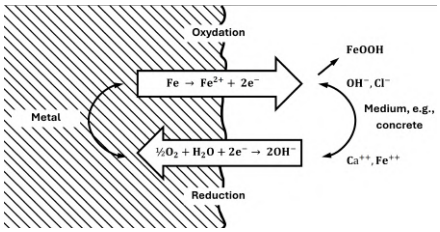

Figure 36: Electrochemical element with reduction reactions at the anode and cathode

4.2 Our experiments

In our experiment, we acidify concrete containing a conductive metal to artificially age it and simulate the conditions of concrete requiring regeneration. Phenolphthalein, a pH indicator, is used to monitor pH variations. In acidic form, phenolphthalein is colorless, but it turns pink when the solution becomes basic. After acidification of the concrete, an attempt is made to restore its basic state through electrolysis. At the beginning, the phenolphthalein should remain colorless, as the mixture is acidic. If the electrolysis works as expected and the pH returns to a basic level, the phenolphthalein will turn pink. The entire process is recorded on video to carefully observe the color change.

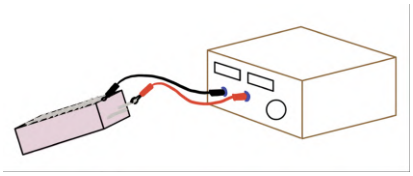

Figure 37: Generator connected to concrete

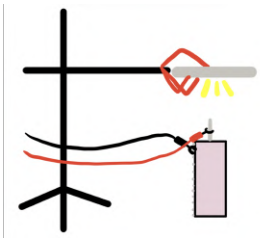

Figure 38: Video capture setup with tripod

Protocol

Fabrication:

- Create a 3 cm thick concrete slab with a U-shaped steel bar of 6 mm diameter (see appendix for the protocol)
- Place a metal mesh on the concrete covered with agar-agar to ensure good distribution of electricity, all wrapped in plastic film.

Aging:

- Acidify the concrete with a hydrochloric acid solution at 1 mol/L (prepared by mixing 200 mL of concentrated hydrochloric acid with 600 mL of water) for 30 minutes.
- Apply phenolphthalein where the steel bar protrudes (this is where the phenomenon will occur).

Restoration:

- Connect the concrete to a generator using wires (and crocodile clips): negative to cathode and positive to anode (the mesh).
- Turn on the generator with a current intensity of 0.4 Ampere at 15 V and wait for the mixture to become basic again.

Record a video to monitor the generation of OH^- ions and their propagation/diffusion over time around the reinforcement, thus allowing calculation of the regeneration speed in cm/min.

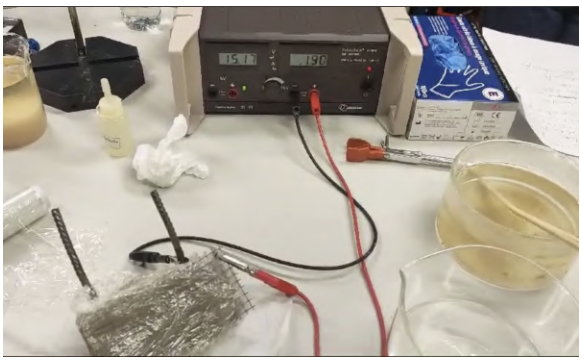

Figure 39: Experimental setup for electrochemical restoration of concrete

4.3 Results

The higher the RGB values, the brighter the color appears. This can be observed during the concrete aging process, which takes about 10 minutes to acidify the surface to a pH below 7, as shown in Figure 40. After 30 minutes, the phenolphthalein indicator becomes completely transparent, signaling that the surface has been sufficiently acidified. It would be relevant to open the concrete further to examine whether the interior has also undergone acidification, as this could provide more detailed information about the state of the material.

In the electrochemical restoration process, the time needed for the electrolysis reaction to move from the reinforcement bar to the mesh is illustrated in Figure 41. It takes about 7 minutes for the reaction to restore a 0.9 cm layer of concrete between the reinforcement bar and the mesh. Extending the electrolysis time would probably be beneficial for additional concrete regeneration, as a longer reaction period would ensure a more complete restoration process, leading to improved durability.

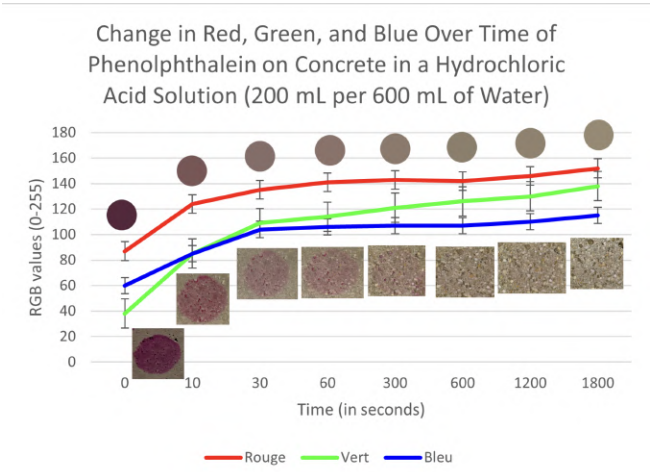

Figure 40: Aging

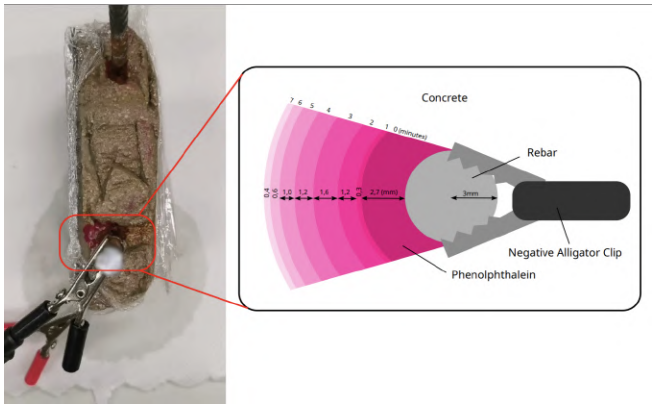

Figure 41: Video monitoring of concrete realkalinization over time: experimental setup (left) and analysis results showing the expansion of the realkalinized zone along the inter-electrode axis (right).

The graph (Figure 42) shows the evolution of the regeneration speed over time, which seems to closely follow an exponential curve, indicating a good fit. This suggests that diffusion processes are the main limiting factor for the regeneration speed. Additionally, the further the area is from the electrode, the more time it takes for regeneration to occur, highlighting the need for patience when seeking to restore areas further away from the source.

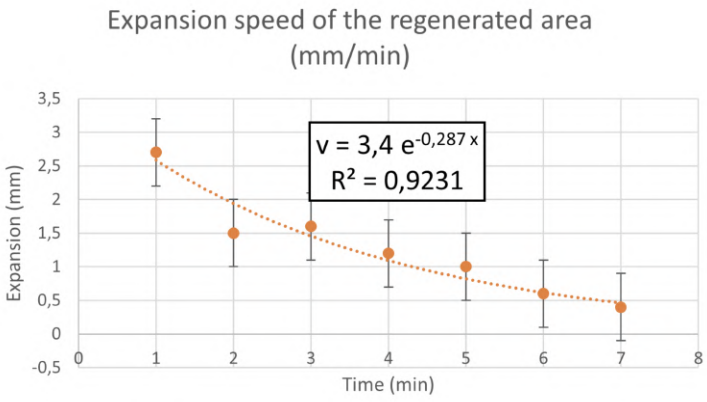

Figure 42: Evolution of the regeneration speed in cm as a function of of distance from the electrode.

5 Implementation of these solutions

5.1 Application of a liquid crystal layer

There is not much to say, it is only necessary to apply a layer of liquid crystal paint over the entire Vauban building. Of course, the diversity of these allows us to not necessarily resort to very visible crystals like green ones. There are liquid crystals whose color change occurs in the ultraviolet domain, much more aesthetic and just as effective.

5.2 Cathodic protection

Main quantities of structural work: Concrete volume: 37,000 m^3, Reinforcement quantities: 5,330 tons, Wall formwork: 63,000 m^2, Slab formwork: 59,000 m^2, Total surface area to be treated: $S = 122,000\,m^2$.

The electrolysis process would require a massive amount of electrical charge to treat the entire concrete structure of the school. However, it is important to note that electrons are produced at the electrode, then must migrate through the concrete, which is a difficult process limiting the efficiency of the technique. In the case of thick walls, as in the Vauban project, this means that ions must travel long distances, further complicating the process.

Given this, the question we must ask ourselves is: knowing that we want to regenerate the Vauban structure in one week, what intensity should we apply?

In this calculation, we will only determine the number of moles of electrons needed for electrolysis over 7 days. This result does not imply that the Vauban structure will actually be regenerated during this period. First, we need to estimate the number of OH^- ions needed for realkalinization. This will give us the number of electrons needed because, according to the half-reaction (equation 7), 1 electron produces 1 OH^- ion.

For reference, in the previous section, the current density was assumed to be $j = 20\,A/m^2$, with 0.4 A for a surface area of $0.02\,m^2$. A lower intensity could extend the time needed for ion migration and achieving the desired regeneration, so we will choose a current density for a real electrolysis treatment.

Current density for electrolysis: $j = 6.25\,A/m^2$, Treatment duration: $\Delta t = 7\,\text{days} = 7 \times 24 \times 3600\,s$.

Step 1: Calculate the total charge (Coulombs) required

We start by calculating the total charge required for the electrolysis process, which will depend on the current density and the duration of treatment.

The total charge Q is given by the equation:

$$Q = j \times S \times \Delta t$$

where:

$$S = 122,000\,m^2 \quad \text{(surface area to be treated)},$$

$$j = 6.25\,A/m^2 \quad \text{(current density)},$$

$$\Delta t = 7 \times 24 \times 3600\,s = 604,800\,s \quad \text{(treatment duration)}.$$

Substituting these values into the equation:

$$Q = 6.25\,A/m^2 \times 122,000\,m^2 \times 604,800\,s = 4.7 \times 10^{13}\,C.$$

Step 2: Calculate the number of electrons transferred

The number of moles of electrons transferred during the electrolysis process can be determined using Faraday's constant, $F = 96,500\,C/mol$.

The number of moles of electrons n is calculated by:

$$n = \frac{Q}{F} = \frac{4.7 \times 10^{13}\,C}{96,500\,C/mol} \approx 4.87 \times 10^{8}\,mol.$$

Step 3: Determine the required current intensity

The next step is to determine the current intensity needed to obtain this charge over the specified period. Using the equation:

$$I = \frac{Q}{\Delta t},$$

we substitute the values:

$$I = \frac{4.7 \times 10^{13}\,\mathrm{C}}{604,800\,\mathrm{s}} \approx 7.78 \times 10^{7}\,\mathrm{A}.$$

Thus, the current intensity required to regenerate the Vauban structure in 1 week is approximately 7.78×10^{7} A.

The electrolysis process would require a massive amount of electrical charge to treat the entire concrete structure of the school. When compared to existing studies on realkalinization by electrolysis, such treatment would be feasible but would require considerable power and time.

Alternative approach: target high-risk areas

APPENDICES

A. Protocol for manufacturing reinforced concrete

For the small concrete block we wish to create, it is preferable to make mortar (without aggregate).

Materials:

- 10 kg bag of mortar
- Water
- Tupperware
- Laser-cut wooden board that adapts to the shape of the Tupperware to make a separator
- Steel rod
- 400 mL beaker
- Spatula
- Lifting support
- Crane and fixing nut

Figure 43: Scale, spatula, U-bars, and beakers

Figure 44: Our mortar mixture

Protocol:

1. Using a scale, weigh 450 g of mortar in a 400 mL beaker.
2. In another beaker, add 100 mL of water and then a few mL of phenolphthalein.
3. Gradually incorporate the mortar into the water, making sure to mix well.
4. The mortar should turn pink, indicating that it is basic.
5. While mixing, prepare the mold for the mortar, which will be part of the Tupperware separated by the wooden board (easy to adjust to get the desired thickness). On the other side, a lifting support will act as a compressor against the board. Using a crane and fixing nut, hold the U-shaped rod in the center of the mold, with the ends pointing upward.
6. Carefully incorporate the mixture into the mold, ensuring all interstices are well filled.
7. Flatten the top and compress with the lifting support.
8. And there you have it! Now just wait more than 24 hours.

B. Python code for an image with a helical step

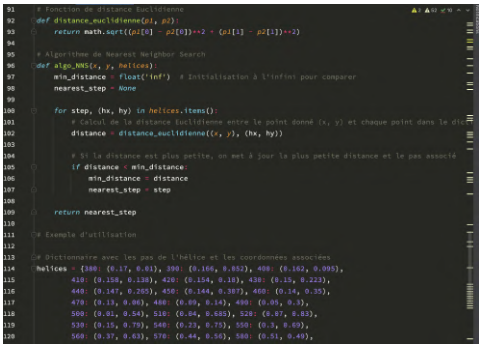

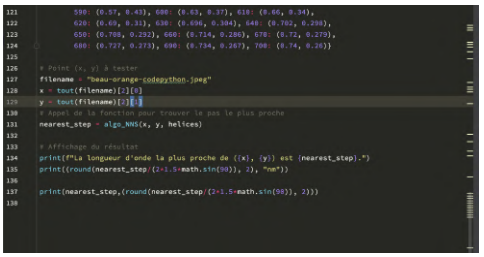

BIBLIOGRAPHY

- P. G. de Gennes, The Physics of Liquid Crystals.
- Sophie Norvez, "Les cristaux liquides: D'un état insoupçonné de la matière aux écrans plats," L'actualité chimique, n°387-388-389, July-October 2014, pp. 148-151.
- Rijeesh Kizhakidathazhath, Yong Geng, Venkata Subba Rao Jampani, Cyrine Charni, Anshul Sharma, and Jan P. F. Lagerwall, "Facile Anisotropic Deswelling Method for Realizing Large-Area Cholesteric Liquid Crystal Elastomers with Uniform Structural Color and Broad-Range Mechanochromic Response," Advanced Functional Materials, vol. 30, no. 7, 2020, DOI: 10.1002/adfm.201909537.
- D.Y. Kim, K.M. Lee, T.J. White, et al., "Cholesteric liquid crystal paints: in situ photopolymerization of helicoidally stacked multilayer nanostructures for flexible broadband mirrors," Nature, NPG Asia Mater 10, 1061–1068 (2018). https://www.nature.com/articles/s41427-018-0096-4.
- Pestana Nakamura, Y., Excerpt from the researcher's thesis, Luxembourg.
- Emmanuel Cailleux and Élisabeth Marie-Victoire, "La réalcalinisation, une nouvelle technique de conservation des monuments historiques en béton armé – Évaluation de l'efficacité, de la durabilité et de l'innocuité des traitements," L'actualité Chimique, n°312-313, October-November, p. 22.
- Valérie L'Hostis, Philippe Dillmann, Walter-John Chitty, Alain Millard and Régis Faquin, "Du Palais des Papes en Avignon au château d'eau Perret à Saclay – Les monuments historiques pour la compréhension du comportement à long terme de l'interface métal/béton," L'actualité Chimique, n°312-313, October-November, p. 17.
- Y. Houst, "Carbonatation du béton et corrosion des armatures," Chantiers/Suisse, vol. 15, n°6, 1984, pp.569-574.
- Réfection des ouvrages en béton, 1994, 145 pages. ISBN 3-905234-85-8. Original edition: ISBN 3-905223471-8. Form. 724.462 f.